Frontiers of Physics
https://doi.org/10.1007/s11467-018-0865-0
Front. Phys.
14(2), 23603 (2019)

RESEARCH ARTICLE

Thermoelectricity in B_{80}-based single-molecule junctions: First-principles investigation

Ying-Xiang Zhen[1,*], **Ming Yang**[2,*], **Rui-Ning Wang**[1,†]

[1] *Hebei Key Lab of Optic-Electronic Information and Materials, College of Physics Science and Technology, Hebei University, Baoding 071002, China*
[2] *Institute of Engineering Thermophysics, Chinese Academy of Sciences, Beijing 100190, China*
Corresponding author. E-mail: [†]*rnwang@hbu.edu.cn*
Received March 25, 2018; accepted September 26, 2018

Thermoelectricity is a thermorelated property that is of great importance in single-molecule junctions. The electrical conductance (σ), electron-derived thermal conductance (κ_{el}) and Seebeck coefficient (S) of B_{80}-based single-molecule junctions are investigated by using density functional theory in combination with non-equilibrium Green's function. When the distance between the left/right electrodes is 11.4 Å, the relationship between σ and κ_{el} obeys the Wiedemann–Franz law very well because of the strong hybridization between B_{80} molecular orbitals and the surface states of Au electrodes. Furthermore, the calculated Lorenz number is close to the famous value in metal or degenerate semiconductors. In addition, S is only -19.09 μV/K at 300 K, thus leading to the smaller electron's thermoelectric figure of merit ($Z_{el}T = S^2\sigma T/\kappa_{el}$). Interestingly, the strain and chemical potential can modulate B_{80}-based single-molecule junctions from n-type to p-type when the compressive strain reaches -0.6 Å or the chemical potential shifts to -0.16 eV. This might be attributed that S reflects the asymmetry in the electrical conductance with respect to the chemical potential and is proportional to the slopes of the transmission spectrum.

Keywords thermoelectricity, single-molecule junction, non-equilibrium Green function

1 Introduction

Since 1974 when Aviram and Ratner firstly proposed a theoretical model of molecular rectifiers [1], molecular electronics have gradually become a cause for concern. Single-molecule junctions show the numerous innovative properties that may be applicable in new forms of electronic devices, such as negative differential resistance, shot noise, and Fano resonances [2–4]. Experimentally, the current–voltage (I–V) characteristics of individual molecules are measured within the mechanically-controllable break junctions or the scanning tunneling microscopes [5, 6]. However, the critical aspects about the electronic structure generally remains unknown by the I–V characteristics alone. Until recently, with the advancement of experimental measurements, not only the electrical conductance ($\sigma = \mathrm{d}I/\mathrm{d}V$) but also the thermopower can be obtained in a modified scanning tunneling microscope [7]. The thermopower can indicate whether single-molecule junctions are p-type or n-type [8].

The thermopower is also called the Seebeck coefficient (S) which, in a linear response regime, can be defined as

$$S = -\frac{\Delta V}{\Delta T}|_{I=0}. \quad (1)$$

ΔV is the voltage counterbalancing the electronic current initiated by a temperature difference (ΔT) across single-molecule junctions. For instance, the measured thermopower of C_{60}-based single-molecule junctions are with a mean value of -18 μV/K by using a scanning tunneling microscope and ~ -14.5 μV/K within the mechanically-controlled break junction [9, 10]. In addition, the "$-$" sign of the Seebeck coefficient implies that the position of the chemical potential of the metal electrodes is closer to the lowest unoccupied molecular orbital (LUMO), namely, the electron is the majority carrier.

Yet, single-molecule junctions offer the promising thermoelectric energy conversion owing to the tunability of their Seebeck coefficients [11–13]. There seems to be a linear dependence of the thermopower with the molecular lengthes for 1, 4-benzenedithiol (8.7 μV/K), 4, 4-dibenzenedithiol (12.9 μV/K), and 4, 4-tribenzenedithiol (14.2 μV/K) molecules [7]. When a C_{60} dimer bridges the gap between Au electrodes, it exhibits negative thermopower values with an average value of -33 μV/K which doubles the magnitude observed in the monomer C_{60}-

*These authors contributed equally to this work.

based junctions [9]. Other than increasing the molecular length, there may be other ways of tuning the thermopower, such as by strengthening the distance between the left/right electrodes or by controlling the chemical potential within a gate [14, 15]. For example, a pure spin thermopower or/and a pure spin current can be obtained by only tuning the gate voltage in a single-molecule-magnet junction [16].

In this manuscript, we choose the B_{80}-based single-molecule junction as a typical model and investigate the effect of the strain as well as the chemical potential and their co-effects on its thermoelectricity. The investigation of thermoelectricity is of crucial significance in the design of the heat-to-electricity generation whose efficiencies are dependent on a dimensionless figure of merit (ZT),

$$ZT = \frac{S^2\sigma T}{\kappa}. \tag{2}$$

Here, κ is the total thermal conductance, which should include all possible contributions (electron (κ_{el}), phonon (κ_{ph}) and other heat carriers (κ_{other}) like photon). To account of the strain-induced modifications of thermoelectric properties of B_{80}-based single-molecule junctions, we carried out σ, S, κ_{el}, as well as $Z_{el}T$ computations by systematically adjusting the closest approaching distance between electrodes. On the other hand, the chemical potential by a gate is an efficient way to adjust the electron and thermal transport in single-molecule junctions [17–19]. Then, in this work we hope to map out the trends by investigating the influence of the strain as well as the chemical potential on the thermoelectric transport through B_{80} molecule. However, a huge number of degrees of freedom in single-molecule junctions cause a particular challeng to establish the general trend.

2 Methodology

The transmission function [$\tau(E)$] is an effective parameter to designate the coherent transport of single-molecule junctions. First of all, a set of functions [$L_\nu(\mu, T)(\nu = 0, 1, 2)$] are introduced as

$$L_\nu(\mu, T) = -\frac{2}{h}\int_{-\infty}^{\infty} \mathrm{d}E(E-\mu)^\nu \tau(E)\frac{\partial f(E,\mu,T)}{\partial E}, \tag{3}$$

with h and $f(E, \mu, T)$ as the Planck constant and Fermi-Dirac distribution, respectively. μ is the chemical potential regulated by a gate in a double-gate experiment [20].

Additionally, σ, S, and κ_{el} are expressed as [21]

$$\sigma = e^2 L_0, \tag{4}$$

$$S = -\frac{1}{eT}\frac{L_1}{L_0}, \tag{5}$$

and

$$\kappa_{el} = -\frac{1}{hT}\left(L_2 - \frac{L_1^2}{L_0}\right), \tag{6}$$

respectively. Obviously, S, σ, and κ_{el} all depend on the electron transport behavior in single-molecule junctions. Actually, they are highly correlated with each other in bulk materials, thus leading to a dire challenge to enhance the thermoelectric figure of merit [22–24].

Lastly, ZT can be obtained by

$$\begin{aligned} ZT &= \frac{S^2\sigma T}{\kappa_{el}+\kappa_{ph}+\kappa_{other}} \\ &= \frac{S^2\sigma T}{\kappa_{el}} \times \frac{\kappa_{el}}{\kappa_{ph}+\kappa_{el}+\kappa_{other}} \\ &= Z_{el}T \times \frac{\kappa_{el}}{\kappa_{ph}+\kappa_{el}+\kappa_{other}}, \end{aligned} \tag{7}$$

where $Z_{el}T$ is completely determined by the electron transmission function. For single-molecule junctions, it is reasonable to assume a vanishing phonon-derived thermal conductance. On one hand, κ_{ph} varies in a wide range of magnitude and is very small in single-molecule junctions [25–27]. On the other hand, the phonon transport is found to play a minor role in the thermal conductance in C_{60}-based single-molecule junctions [28]. In comparison with C_{60}-based single-molecule junctions, B_{80}-based single-molecule junctions have a better electron transport behavior due to the strong coupling between B_{80} molecules and metal electrodes. Therefore, $Z_{el}T$ can be used to qualitatively describe the thermoelectric performance of B_{80}-based single-molecule junctions. In addition, electron-vibration coupling is not taken into consideration, which typically tend to reduce the thermoelectric efficiency [29, 30].

$\tau(E)$ was calculated by using the non-equilibrium Green's function method as realized in the SMEAGOL package [31, 32]. The norm-conserving Troullier-Martins pseudopotential is applied to describe the core electrons [33, 34]. The exchange-correlation functional is described by the Perdew-Burke-Ernzerhof parametrization of generalised gradient approximation [35]. The valence electrons are expanded in double zeta plus the polarized basis sets. The Brillouin zone has been sampled with $1\times1\times10$ points within the Monkhorst–Pack sampling scheme [36]. The electrostatic potentials are determined on a real-space grid with a mesh cutoff energy of 300 Ry.

3 Result and discussion

As sketched in Fig. 1(a), a B_{80} molecule is rigidly connected to two semi-infinite Au(100) nano-electrodes. In addition, both the planar surfaces of electrodes are taken into consideration. To start with, the total energy-distance calculations were executed and are shown in Fig. 1(b). It is found that the connection between the total energy and the distance between the left/right electrodes is parabolic when the distance is in the range from 11.0 Å to 12.2 Å. That is, in this range the deformation remains as an elastic deformation. When the distance is less than 11.0 Å,

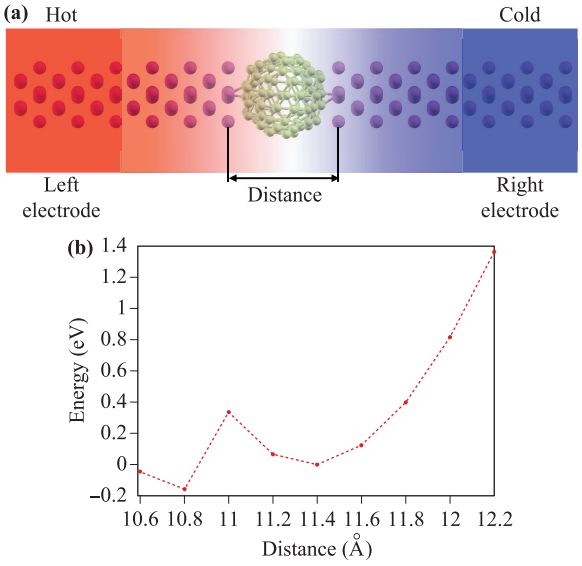

Fig. 1 **(a)** Schematic illustration of a B_{80} molecule connected to the left/right Au(100) nano-electrodes. **(b)** The total energies as a function of the distance between the left/right electrodes.

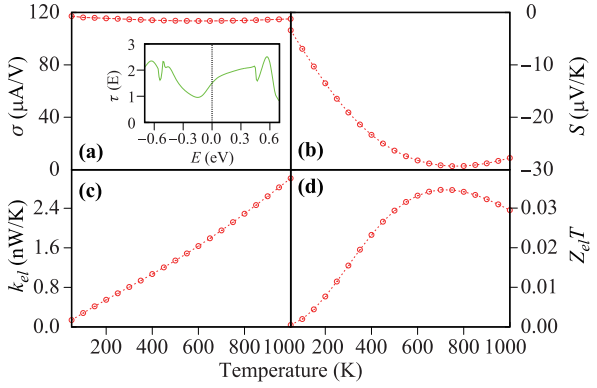

Fig. 2 Electrical conductances (σ) **(a)**, Seebeck coefficients (S) **(b)**, electron-derived thermal conductances (κ_{el}) **(c)** and the thermoelectric figure of merits ($Z_{el}T$) **(d)** vs. the temperature (T) from 50 to 1000 K in B_{80}-based single-molecule junctions. Inside of (a), the transmission spectrum with the energy is illustrated at 300 K. The zero energy is chosen at the chemical potential of metal electrodes.

the single-molecule junction is in the plastic deformation, thus resulting in a decreased total energy. Consequently, it is assumed that the equilibrium distance between the left and right electrodes is 11.4 Å.

Experimentally, the ambient temperature (T) of single-molecule junctions is changeable. Consequently, we investigate σ, S, κ_{el}, and $Z_{el}T$ as a function of the temperature (T) from 50 to 1000 K, which are displayed in Fig. 2. Note that the distance between the left/right electrode is fixed to 11.4 Å. As presented in Fig. 2(a) and (c), σ is insensitive to T while κ_{el} boosts linearly with the rising of T. Particularly, κ_{el} increases from 0.14 nW/K to 3.01 nW/K when T ascends from 50 K to 1000 K. Actually, σ and κ_{el} correlate to each other and are constrained by a Lorenz number (L) within the Wiedemann–Franz law ($\kappa_{el} = L \cdot \sigma \cdot T$). The obtained L is approximately 2.43×10^{-8} W·Ω/K^2 and is very close to the famous value ($\sim 2.45 \times 10^{-8}$ W·Ω/K^2) in metals or degenerate semiconductors. This is because B_{80}-based single-molecule junction has a well-behaved electrical conductivity which can be seen from $\tau(E)$, as appeared in the inset of Fig. 2(a). From Fig. 2(b), the sign of S is negative. That is, the electrons are the majority carriers. In addition, the absolute S increases with T increasing and reach its maximum ($\sim$ 29.32 μV/K) at 750 K, which is typically rather low and comparable to the measured S in C_{60}-based single-molecule junctions [9, 10]. Additionally, $Z_{el}T$ in B_{80}-based single-molecule junctions reaches the maximum at 700 K and is about 0.035. In other words, the thermoelectric performance of B_{80}-based single-molecule junction is very poor, because the relationship between σ and κ_{el} is bound by the Wiedemann–Franz law [23]. Furthermore, the Wiedemann–Franz law is proved to be invalid in a single-electron and Fano-resonant junctions, further leading to a better thermoelectric performance [37–40].

In B_{80}-based single-molecule junctions, the strain can be termed as the difference between the electrode-electrode distance and its equilibrium distance ($\sim$ 11.4 Å). The negative sign suggests a compressive strain and the positive value implies the tensile strain. In this work, the strain is in the range of $[-0.8, 0.8]$ Å. Though there is a plastic deformation in case that the compressive strain surpasses −0.6 Å, the junctions are stable in this region. As depicted in Figs. 3(a) and (c), σ and κ_{el} are also severely dependent on the tensile/compressive strain in B_{80}-based single-molecule junction as in C_{60}-based single-molecule junction [41]. They goes up at the same time when the strain declines from the tensile (0.8 Å) to compressive (−0.8 Å) strain, because the strain provokes the enhancement of the contact coupling between B_{80} molecules and Au electrodes. σ changes from 66.74 μA/V (0.8 Å) to 171.26 μA/V (−0.8 Å) and κ_{el} increases from 0.52 nW/K (0.8 Å) to 1.12 nW/K (−0.8 Å).

In general, the effect of the strain on the thermopower is very complicated in B_{80}-based single-molecule junction, as shown in Fig. 3(b). However, both the experimental measurements and theoretical calculations show that S will escalate considerably with increasing the electrode-electrode distance in a benzene-1, 4-dithiolate single-molecule junction [14, 15]. In B_{80}-based single-molecule junction, the absolute S decreases when the strain increases from 0.2 Å to 0.8 Å and decreases from 0.2 Å to −0.4 Å, respectively. Unexpectedly, the sign of S changes into "+" when the compressive strain is −0.6 Å. And then, the sign of S changes back into "−" under −0.8 Å compressive strain. That is, B_{80}-based single-molecule junction can be changed from n-type to p-type and then to n-type

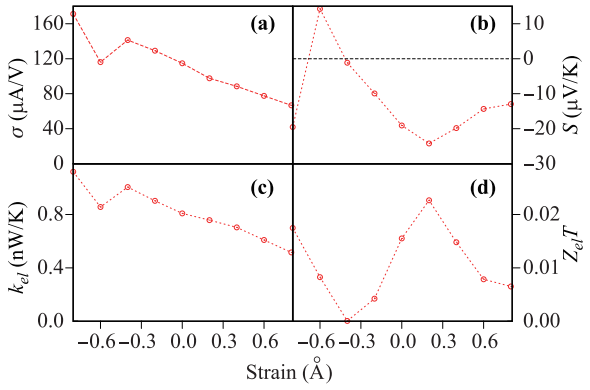

Fig. 3 Electrical conductances (σ) **(a)**, Seebeck coefficients (S) **(b)**, electron-derived thermal conductances (κ_{el}) **(c)** and the thermoelectric figure of merits ($Z_{el}T$) **(d)** vs. the strain from −0.8 Å to 0.8 Å in B_{80}-based single-molecule junctions at 300 K.

by utilizing a compressive strain. The absolute S has a maximum value (~ -24.21 μV/K) at 0.2 Å tensile strain and its corresponding maximum $Z_{el}T$ values are 0.023, as shown in Fig. 3(d). As a result, the strain can be used to modulate the thermoelectric transport properties of single-molecule junctions, but its effect is more complex.

In order to resolve the influence of the strain in detail, the transmission spectra *via* the strain are shown in Fig. 4. As the strain diminishes from 0.8 to −0.4 Å, there are a few common characteristics in the variation of transmission spectra: the LUMO shifts to the chemical potential of metal electrodes and becomes more and more broadened as a result of the enhanced hybridization between B_{80} molecular orbitals and the surface states of left/right electrodes [42]. Therefore, σ and κ_{el} increase in B_{80}-based single-molecule junctions when the strain shifts from 0.8 Å tensile strain to −0.4 Å compressive strain. In addition, S can be further simplified using the Sommerfeld expansion as

$$S = -\frac{\pi^2 \kappa_B^2 T}{3e} \frac{\partial ln\tau(E)}{\partial E} \mid_{E=E_f} . \tag{8}$$

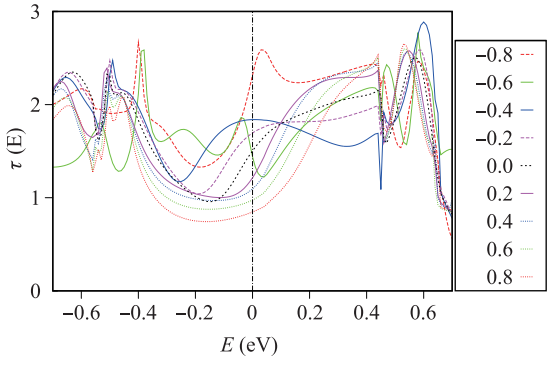

Fig. 4 Transmission spectra vs. the strain from −0.8 to 0.8 Å in B_{80}-based single-molecule junctions. The solid lines represent some specific spectra. The zero energy is chosen at the chemical potential of metal electrodes.

Obviously, S is related not only to the magnitude but also to the slope of $\tau(E)$ in the vicinity of the Fermi level. Here, the maximum absolute S locates at 0.2 Å tensile strain instead of −0.4 Å compressive strain where a transmission peak locates at the chemical potential of metal electrodes. When the strain is in the range $[-0.4, 0.8]$ Å, S is "−" because $\partial\tau(E)/\partial E|_{E=E_f} > 0$. On the contrary, S is "+" because $\partial\tau(E)/\partial E|_{E=E_f} < 0$ at −0.6 Å compressive strain.

From the above-mentioned equations, σ, S, and κ_{el} are governed by the chemical potential (μ), which can be controllably adjusted by a gate in the dual-gate experiments [17, 18, 20]. Therefore, for the equilibrium B_{80}-based single-molecule junction we illustrate the changes of the thermoelectric properties as a function of μ in Fig. 5. Obviously, as shown in the (a) and (c) panels, μ induces σ and κ_{el} change along evenly together. When μ shifts to −0.16 eV, the minimum σ and κ_{el} are 39.11 μA/V and 0.32 nW/K, respectively. Accordingly, the effect of μ on the thermoelectric performance in B_{80}-based single-molecule junctions chiefly rely on the changes of S along with μ. As shown in Fig. 5(b), the results show that the characteristics of S are sensitive to μ. The most striking feature is that the B_{80}-based single-molecule junctions can be transformed from n-type to p-type by shifting μ. S is close to zero when μ shifts to −0.16 eV. This can be noticeably comprehended from the transmission spectrum, as revealed in the inside panel of Fig. 2(a). A valley appears at −0.16 eV in the transmission function. As μ further decreases, the sign of S becomes "+" (p-type) because $\partial\tau(E)/\partial E|_{E=E_f} < 0$. The maximum S are 23.56 μV/K and −22.77 μV/K in case that μ shifts to −0.35 eV and −0.05 eV, respectively. The corresponding maximum $Z_{el}T$ [Fig. 5(d)] are 0.023 and 0.021, respectively.

Finally, we consider the combined action of the strain and the chemical potential on the thermopower and thermoelectric figure of merit, as shown in Fig. 6. From Fig. 6(a), when μ shifts to about −0.4 eV, the maximum

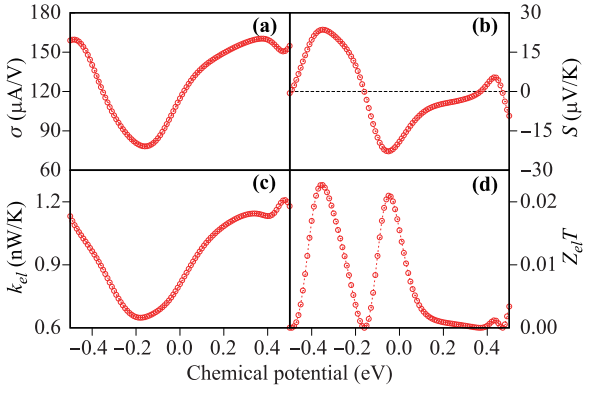

Fig. 5 Electric conductances (σ) **(a)**, Seebeck coefficients (S) **(b)**, electron-derived thermal conductances (κ_{el}) **(c)** and the thermoelectric figure of merits ($Z_{el}T$) **(d)** vs. the chemical potential from −0.5 eV to 0.5 eV in B_{80}-based single-molecule junctions at 300 K.

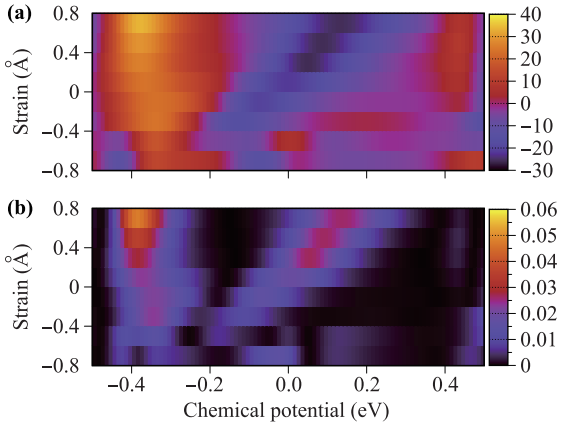

Fig. 6 Seebeck coefficients [S (μV/K)] **(a)** and the thermoelectric figure of merits ($Z_{el}T$) **(b)** under the co-action of the strain and the chemical potential in B_{80}-based single-molecule junctions at 300 K.

positive S are obtained, irrespective of the strain applied to B_{80}-based single-molecule junction. On the other hand, as the strain increases from −0.4 Å to 0.8 Å, the minimum negative S locates from −0.14 eV to 0.16 eV. In general, the maximum positive and minimum negative thermopower are 36.28 μV/K and −26.07 μV/K under 0.8 Å tensile strain when μ shifts to −0.38 eV and 0.16 eV, respectively. The corresponding $Z_{el}T$ are 0.054 and 0.027, as displayed in Fig. 6(b). In comparison with the equilibrium case, it can be increased a two-fold by the co-action of the strain and the chemical potential.

4 Summary

By utilizing density functional theory together with non-equilibrium Green's function, the thermoelectric properties of B_{80}-based single-molecule junctions are explored by taking into consideration the effects of the temperature, the strain and the chemical potential. Mostly, the calculated thermoelectric figure of merit ($Z_{el}T$) is rather small. There are two reasons for this. First, the coupling between B_{80} molecule and Au electrodes is robust and the transmission spectrum is expanded, thus leading to a smaller Seebeck coefficient. Second, the relationships between σ and κ_{el} obey the Wiedemann–Franz law very well and the Lorenz number is close to the famous value in metals or degenerate semiconductors. In response, some works recommend to improve the thermoelectric performance by violating the Wiedemann–Franz law due to Fano effect [38–40] or reducing the Lorenz number due to pudding mold type band structures [43].

Acknowledgements This work was supported by the National Natural Science Foundation of China under Grant Nos. 61704044, 11547170, 51772297, and 11464052, the Natural Science Foundation of Hebei Province under Grant No. A2017201219, and the Educational Commission of Hebei Province under Grant No. ZD2018030. The calculations were supported by the High-Performance Computing Center of Hebei University and the Institute of Engineering Thermophysics, Chinese Academy of Sciences.

References

1. A. Aviram and M. A. Ratner, Molecular rectifiers, *Chem. Phys. Lett.* 29(2), 277 (1974)
2. X. Zheng, W. Lu, T. A. Abtew, V. Meunier, and J. Bernholc, Negative differential resistance in C_{60}-based electronic devices, *ACS Nano* 4(12), 7205 (2010)
3. R. Liu, S.H. Ke, H. U. Baranger, and W. Yang, *J. Am. Chem. Soc.* 128, 2074 (2005)
4. T. A. Papadopoulos, I. M. Grace, and C. J. Lambert, Control of electron transport through Fano resonances in molecular wires, *Phys. Rev. B* 74(19), 193306 (2006)
5. W. Wang, T. Lee, and M. A. Reed, Mechanism of electron conduction in self-assembled alkanethiol monolayer devices, *Phys. Rev. B* 68(3), 035416 (2003)
6. H. Song, M. A. Reed, and T. Lee, Single molecule electronic devices, *Adv. Mater.* 23(14), 1583 (2011)
7. P. Reddy, S. Y. Jang, R. A. Segalman, and A. Majumdar, Thermoelectricity in molecular junctions, *Science* 315(5818), 1568 (2007)
8. M. Paulsson and S. Datta, Thermoelectric effect in molecular electronics, *Phys. Rev. B* 67(24), 241403 (2003)
9. C. Evangeli, K. Gillemot, E. Leary, M. T. Gonz'alez, G. Rubio-Bollinger, C. J. Lambert, and N. Agraït, Engineering the thermopower of C_{60} molecular junctions, *Nano Lett.* 13(5), 2141 (2013)
10. S. K. Yee, J. A. Malen, A. Majumdar, and R. A. Segalman, Thermoelectricity in fullerene–metal heterojunctions, *Nano Lett.* 11(10), 4089 (2011)
11. F. Hüser and G. C. Solomon, *J. Phys. Chem. C* 119, 14056 (2015)
12. Y. Dubi and M. Di Ventra, *Colloquium*: Heat flow and thermoelectricity in atomic and molecular junctions, *Rev. Mod. Phys.* 83(1), 131 (2011)
13. A. Shakouri, Recent developments in semiconductor thermoelectric physics and materials, *Annu. Rev. Mater. Res.* 41(1), 399 (2011)
14. M. Tsutsui, T. Morikawa, Y. He, A. Arima, and M. Taniguchi, High thermopower of mechanically stretched single-molecule junctions, *Sci. Rep.* 5(1), 11519 (2015)
15. A. Torres, R. B. Pontes, A. J. R. da Silva, and A. Fazzio, Tuning the thermoelectric properties of a single-molecule junction by mechanical stretching, *Phys. Chem. Chem. Phys.* 17(7), 5386 (2015)
16. R. Q. Wang, L. Sheng, R. Shen, B. Wang, and D. Y. Xing, Thermoelectric effect in single-molecule-magnet junctions, *Phys. Rev. Lett.* 105(5), 057202 (2010)
17. K. Yoshida, L. Hamada, S. Sakata, A. Umeno, M. Tsukada, and K. Hirakawa, Gate-tunable large negative tunnel magnetoresistance in Ni–C_{60}–Ni single molecule transistors, *Nano Lett.* 13(2), 481 (2013)

18. A. Tan, J. Balachandran, S. Sadat, V. Gavini, B. D. Dunietz, S. Y. Jang, and P. Reddy, Effect of length and contact chemistry on the electronic structure and thermoelectric properties of molecular junctions, *J. Am. Chem. Soc.* 133(23), 8838 (2011)
19. Y. S. Liu and Y. C. Chen, Seebeck coefficient of thermoelectric molecular junctions: First-principles calculations, *Phys. Rev. B* 79(19), 193101 (2009)
20. I. Pallecchi, F. Telesio, D. Li, A. Fête, S. Gariglio, J. M. Triscone, A. Filippetti, P. Delugas, V. Fiorentini, and D. Marré, Giant oscillating thermopower at oxide interfaces, *Nat. Commun.* 6(1), 6678 (2015)
21. U. Sivan and Y. Imry, Multichannel Landauer formula for thermoelectric transport with application to thermopower near the mobility edge, *Phys. Rev. B* 33(1), 551 (1986)
22. X. Shi, L. D. Chen, S. Q. Bai, X. Y. Huang, X. Y. Zhao, Q. Yao, and C. Uher, Influence of fullerene dispersion on high temperature thermoelectric properties of $Ba_yCo_4Sb_{12}$-based composites, *J. Appl. Phys.* 102(10), 103709 (2007)
23. C. A. Perroni, D. Ninno, and V. Cataudella, Electron-vibration effects on the thermoelectric efficiency of molecular junctions, *Phys. Rev. B* 90(12), 125421 (2014)
24. G. D. Mahan and J. O. Sofo, The best thermoelectric, *Proc. Natl. Acad. Sci. USA* 93(15), 7436 (1996)
25. Y. S. Liu, B. C. Hsu, and Y. C. Chen, Effect of thermoelectric cooling in nanoscale junctions, *J. Phys. Chem. C* 115(13), 6111 (2011)
26. Z. Wang, J. A. Carter, A. Lagutchev, Y. K. Koh, N. H. Seong, D. G. Cahill, and D. D. Dlott, Ultrafast flash thermal conductance of molecular chains, *Science* 317(5839), 787 (2007)
27. T. Shiota, A. I. Mares, A. M. C. Valkering, T. H. Oosterkamp, and J. M. van Ruitenbeek, Mechanical properties of Pt monatomic chains, *Phys. Rev. B* 77(12), 125411 (2008)
28. J. C. Klöckner, R. Siebler, J. C. Cuevas, and F. Pauly, Thermal conductance and thermoelectric figure of merit of C_{60}-based single-molecule junctions: Electrons, phonons, and photons, *Phys. Rev. B* 95(24), 245404 (2017)
29. C. A. Perroni, D. Ninno, and V. Cataudella, Thermoelectric efficiency of molecular junctions, *J. Phys.: Condens. Matter* 28(37), 373001 (2016)
30. B. C. Hsu, C. W. Chiang, and Y. C. Chen, Effect of electron–vibration interactions on the thermoelectric efficiency of molecular junctions, *Nanotechnology* 23(27), 275401 (2012)
31. Y. Xue, S. Datta, and M. A. Ratner, First-principles based matrix Green's function approach to molecular electronic devices: general formalism, *Chem. Phys.* 281(2–3), 151 (2002)
32. A. R. Rocha, V. M. García-Suárez, S. Bailey, C. Lambert, J. Ferrer, and S. Sanvito, Spin and molecular electronics in atomically generated orbital landscapes, *Phys. Rev. B* 73(8), 085414 (2006)
33. D. R. Hamann, M. Schlüter, and C. Chiang, Norm-conserving pseudopotentials, *Phys. Rev. Lett.* 43(20), 1494 (1979)
34. N. Troullier and J. L. Martins, Efficient pseudopotentials for plane-wave calculations, *Phys. Rev. B* 43(3), 1993 (1991)
35. J. P. Perdew, K. Burke, and M. Ernzerhof, Generalized gradient approximation made simple, *Phys. Rev. Lett.* 77(18), 3865 (1996)
36. H. J. Monkhorst and J. D. Pack, Special points for Brillouin-zone integrations, *Phys. Rev. B* 13(12), 5188 (1976)
37. B. Kubala, J. König, and J. Pekola, Violation of the Wiedemann–Franz law in a single-electron transistor, *Phys. Rev. Lett.* 100(6), 066801 (2008)
38. G. Gómez-Silva, O. Ávalos-Ovando, M. L. Ladrón de Guevara, and P. A. Orellana, Enhancement of thermoelectric efficiency and violation of the Wiedemann–Franz law due to Fano effect, *J. Appl. Phys.* 111(5), 053704 (2012)
39. R. N. Wang, G. Y. Dong, S. F. Wang, G. S. Fu, and J. L. Wang, Impact of contact couplings on thermoelectric properties of anti, Fano, and Breit-Wigner resonant junctions, *J. Appl. Phys.* 120(18), 184303 (2016)
40. R. Stadler and T. Markussen, Controlling the transmission line shape of molecular t-stubs and potential thermoelectric applications, *J. Chem. Phys.* 135(15), 154109 (2011)
41. N. Hauptmann, F. Mohn, L. Gross, G. Meyer, T. Frederiksen, and R. Berndt, Force and conductance during contact formation to a C_{60} molecule, *New J. Phys.* 14(7), 073032 (2012)
42. K. S. Thygesen and A. Rubio, Renormalization of molecular quasiparticle levels at metal-molecule interfaces: Trends across binding regimes, *Phys. Rev. Lett.* 102(4), 046802 (2009)
43. H. Usui and K. Kuroki, Enhanced power factor and reduced Lorenz number in the Wiedemann–Franz law due to pudding mold type band structures, *J. Appl. Phys.* 121(16), 165101 (2017)